Use of In-Situ Observations of Arctic Clouds to Understand Impacts of Mixed-Phase Clouds on Single-Scattering Properties: Applications to Climate Models

G. M. McFarquhar and G. Zhang
University of Illinois
Department of Atmospheric Sciences
Urbana, Illinois

S. Cober
Clouds Physics Research Division
Meteorological Service of Canada
Downsview, Ontario

Introduction

Complex feedback mechanisms involving sea ice, snow cover, and clouds must be better understood and characterized before large disagreements between general circulation model (GCM) simulations of Arctic conditions can be reduced and future predictions of climate change refined. Observations obtained during the First International Satellite Cloud Climatology Project (ISCCP) Regional Experiment (FIRE) Arctic Clouds Experiment (ACE) and during the Surface Heat Budget of the Arctic Ocean Experiment (SHEBA) are used here to enhance our understanding of mass and single-scattering properties of mixed-phase Arctic clouds and their influence on energy budgets.

For Arctic clouds, Shupe et al. (2001) showed that retrieval techniques for all-ice and all-liquid clouds could be used only 34% of the time, suggesting mixed-phase clouds or overlapping clouds were present at other times. In this study, in-situ measurements of cloud properties obtained during SHEBA and FIRE.ACE are used to examine the contributions of water and ice to mixed-phase single-scattering properties and to investigate the manner in which these phases mix.

In-Situ Instruments

Data collected by in-situ microphysical probes on board the National Center for Atmospheric Research (NCAR) C-130 and the National Research Council (NRC) Convair-580 during May and July of 1998 are used. Over 120 minutes of data were collected in mixed-phase clouds, defined to be 30-s time intervals when both liquid and ice were detected with in-situ probes. Using some modifications to Cober et al. (2001) techniques, phase is identified using observations of hydrometeor shapes obtained by standard two-dimensional (2D) cloud and precipitation probes and a Cloud Particle Imager (CPI), measurements of supercooled water by a Rosemount icing detector (RICE) and a Nezvorov probe, and observations of small particle size distributions obtained by forward scattering spectrometer probes (FSSPs).

Figure 1 shows ice crystals measured by a CPI in a mixed-phase cloud penetrated by the C-130. The larger non-spherical crystal images, combined with a response from the RICE to smaller supercooled water drops, proved that this was a mixed-phase cloud. Estimates of ice mass from mass-diameter relationships applied to ice concentrations estimated from the 2D probe and of water mass from concentrations of supercooled water drops measured by the FSSP and RICE showed that mass was dominated by ice at this time.

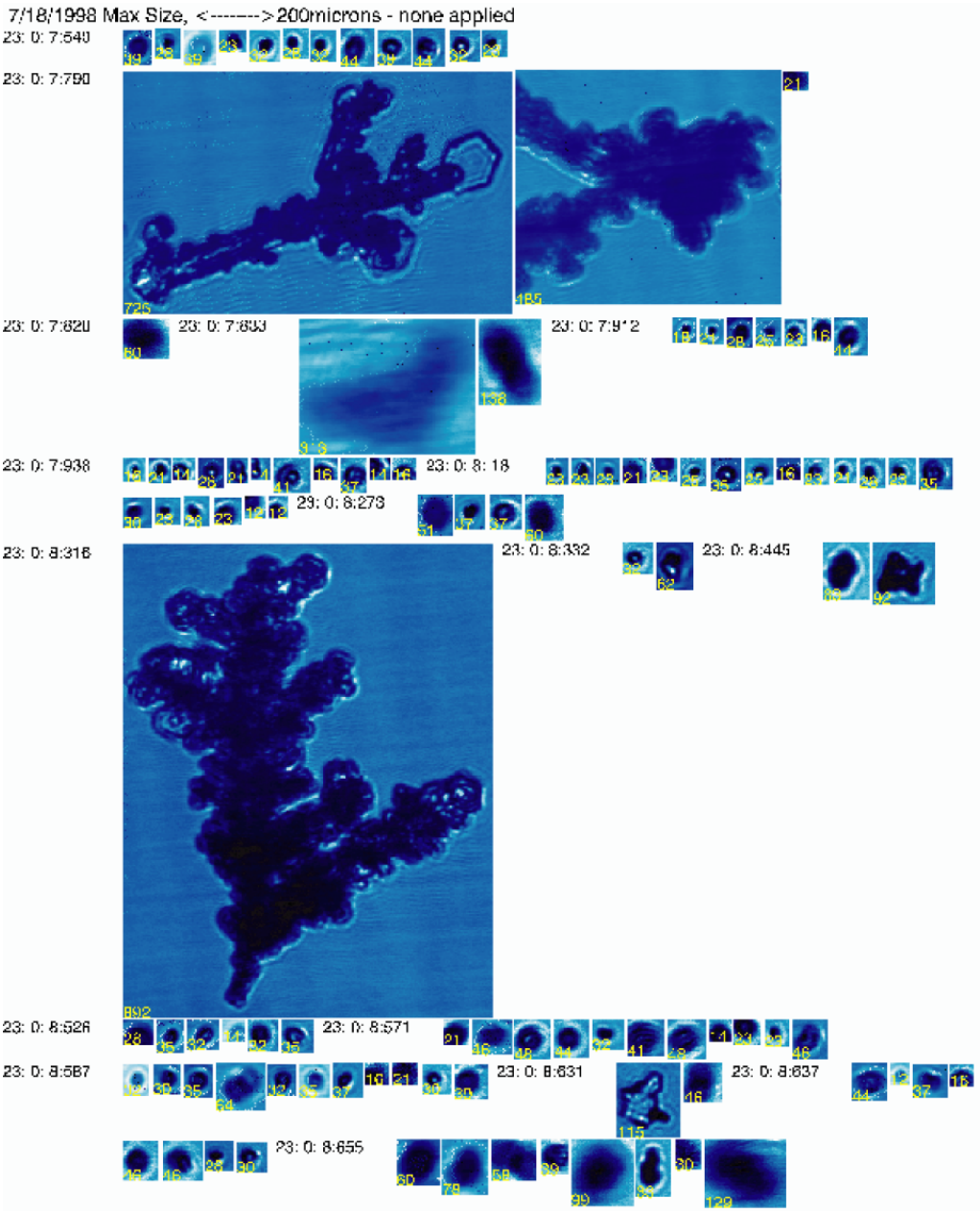

Figure 1. Observations of cloud particles made by CPI in mixed-phase cloud during flight of NCAR C-130, July 18, 1998. Observations made during time period where ice dominated mass concentrations.

Approximately 2 minutes later, the C-130 penetrated a portion of cloud dominated by small liquid drops, when only one large ice crystal in the CPI data and only a few ice crystals in the 2D data were seen in a 45 second time period. Examples of crystal images for this time period are shown in Figure 2.

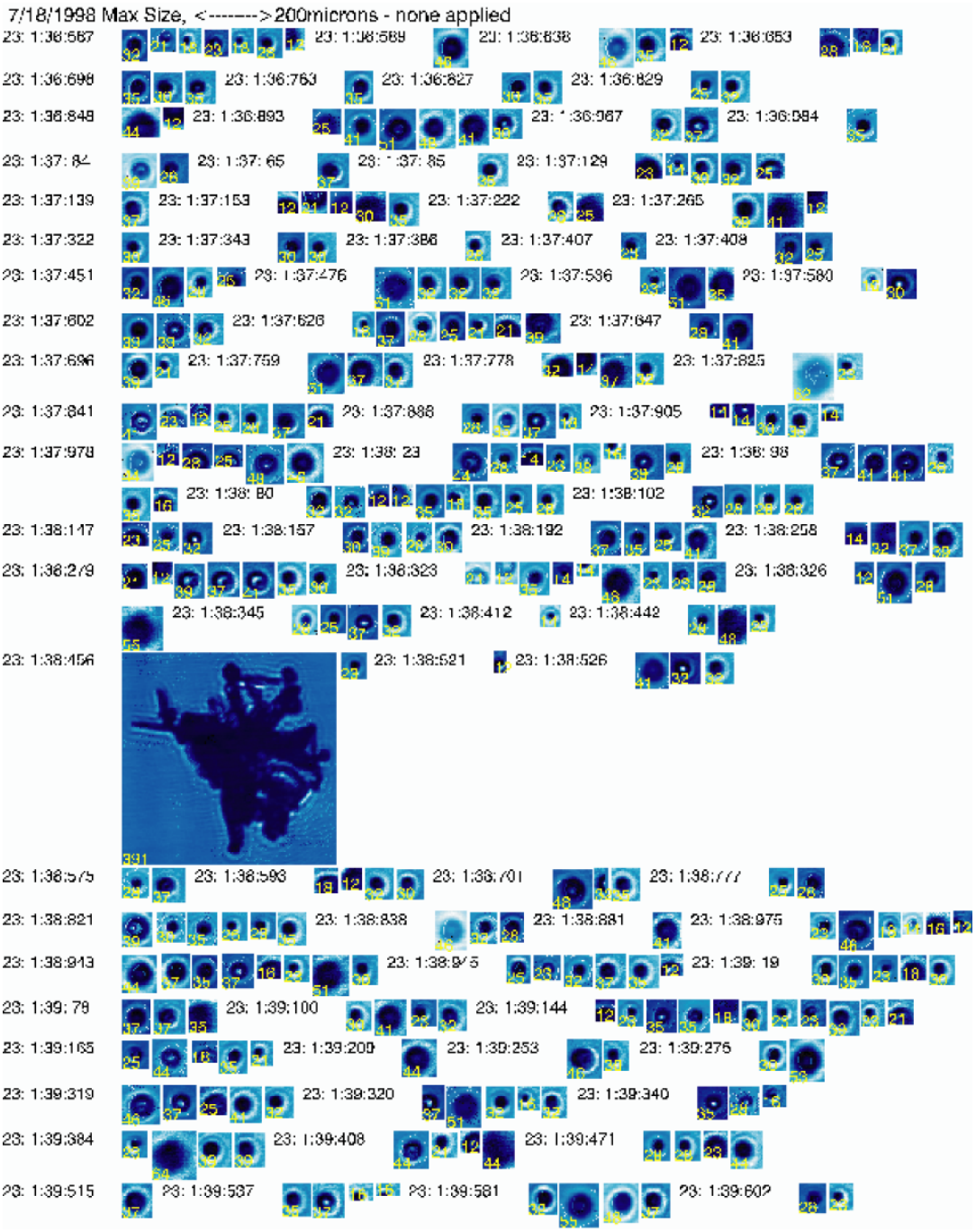

Figure 2. Observations of cloud particles made by CPI in mixed-phase cloud during flight of NCAR C-130, July 18, 1998. Observations made during time period where small liquid drops dominated mass concentrations.

A statistical analysis was performed to determine if mixed-phase clouds, in general, consisted of regions alternately dominated by water and ice. Figure 3 shows contributions of liquid to total mass, f_l, based on Nezvorov probe measurements, for all mixed-phase clouds penetrated by the Convair. The clustering of points about f_l=1 shows that for many cases, independent of temperature, IWCs are too small to be measured by the Nezvorov probe. Note that when average f_l is computed for all clouds (ice, liquid, and mixed-phase) measured, the clustering around f_l=1 disappears.

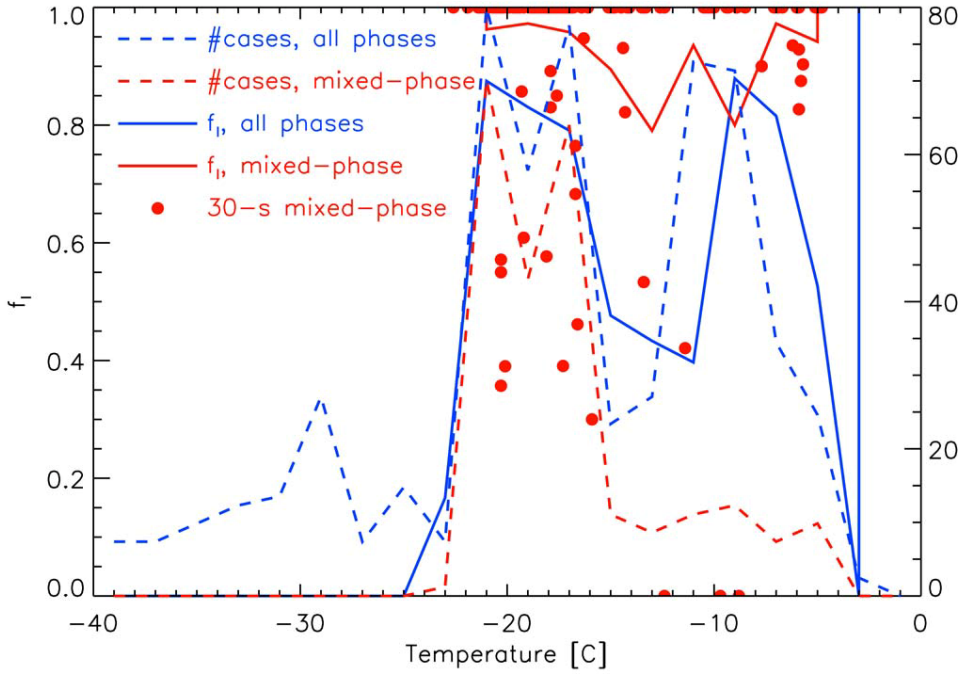

Figure 3. Average fraction of liquid in mixed-phase clouds, f_l, and number of 30-s in-cloud time periods as function of temperature based on data acquired by the NRC Convair-580. Thin lines correspond to data collected in all (liquid-, ice-, and mixed-phase) cloud types, whereas thick lines correspond to only mixed-phase clouds. Solid circles correspond to f_l calculated for each 30-s period in mixed-phase cloud.

Figure 4, based on observations collected by the NCAR C-130, further shows that most mixed-phase clouds have the majority of mass contained in either ice crystals or supercooled water droplets. Analysis from the Convair data suggests that 87% of mixed clouds have more than 90% of their mass content contained in supercooled droplets. Cober et al. (2001) and Korolev et al. (2003) have collected substantial data in mixed-phase clouds, showing that approximately 80% of mixed-phase clouds, on average, have ice fractions of either greater than 0.9 or less than 0.1.

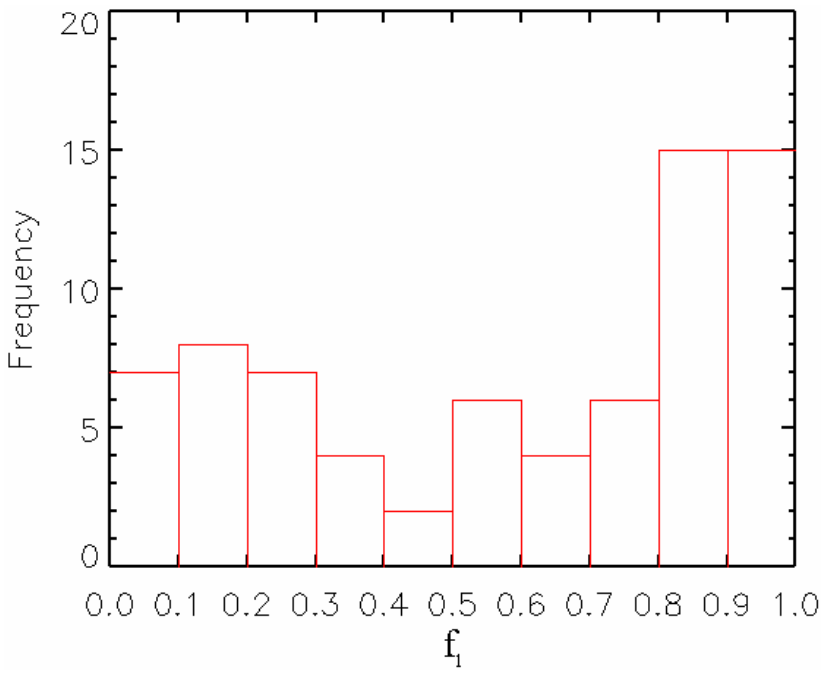

Figure 4. Frequency of occurrence of fraction of liquid in mixed-phase clouds, where fractions computed by averaging liquid and ice size distributions over a 30 s in-cloud time periods (based on data acquired by NCAR C-130).

Computed Scattering Properties of Mixed-Phase Clouds

Computations were performed to investigate whether this clustering of water and ice in mixed-phase clouds causes the scattering properties to differ from those calculated using parameterization schemes based on average amounts of water and ice over all phases of clouds. To do this, number concentrations of larger ice particles from 2D data and of supercooled water droplets from FSSP data are determined following McFarquhar and Cober (2004). The mean single-scattering properties (single-scatter albedo ω_0, asymmetry parameter g, scattering phase function $P(\Theta)$), are computed by weighting the analogous property of individual water droplets, computed from Mie theory, or ice crystals, computed by improved geometric optics, (Yang et al. 2000), by number concentration and scattering cross-section. Figure 5 shows examples of ice crystals imaged in mixed-phase clouds. Because of the variety of shapes observed, a habit classification scheme determines which crystal shape (e.g., dendrite, needle, aggregate) is to be used to compute scattering properties for each time interval.

Figure 6 shows frequency distributions of β_{ext} calculated in this way, different line types representing mixed-, liquid- and ice-phase clouds; for ice clouds, calculations both with and without contributions due to small crystals measured by the FSSP are shown. As expected, due to the dominance of supercooled droplets in mixed-phase clouds, β_{ext} for water and mixed-phase clouds are larger than those for ice clouds, even when small ice crystals are assumed to have the concentrations measured by the FSSP, presumably representing an upper bound.

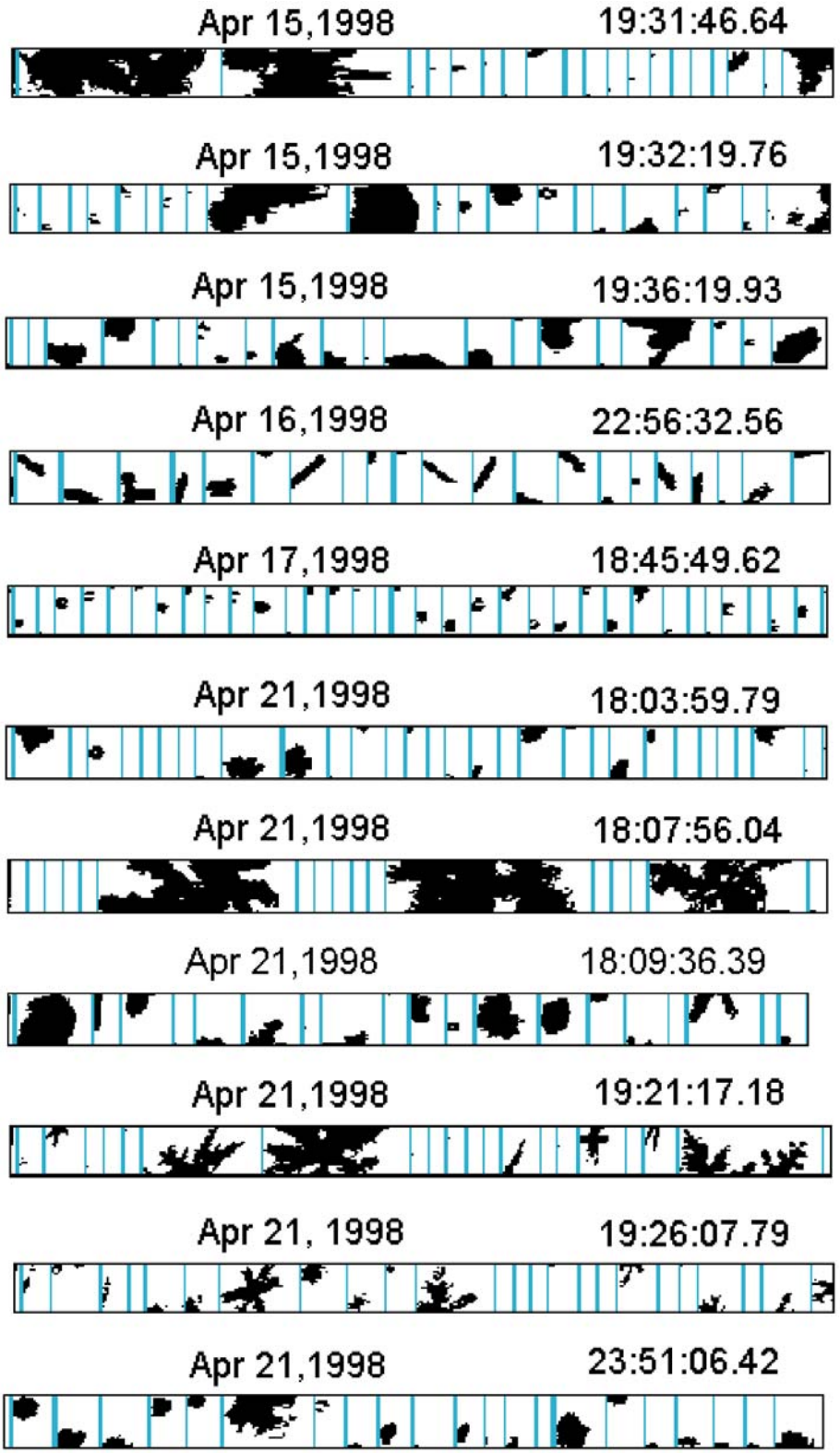

Figure 5. Crystals imaged by 2D probes in conditions identified as mixed-phase by Cober et al. (2001) algorithm.

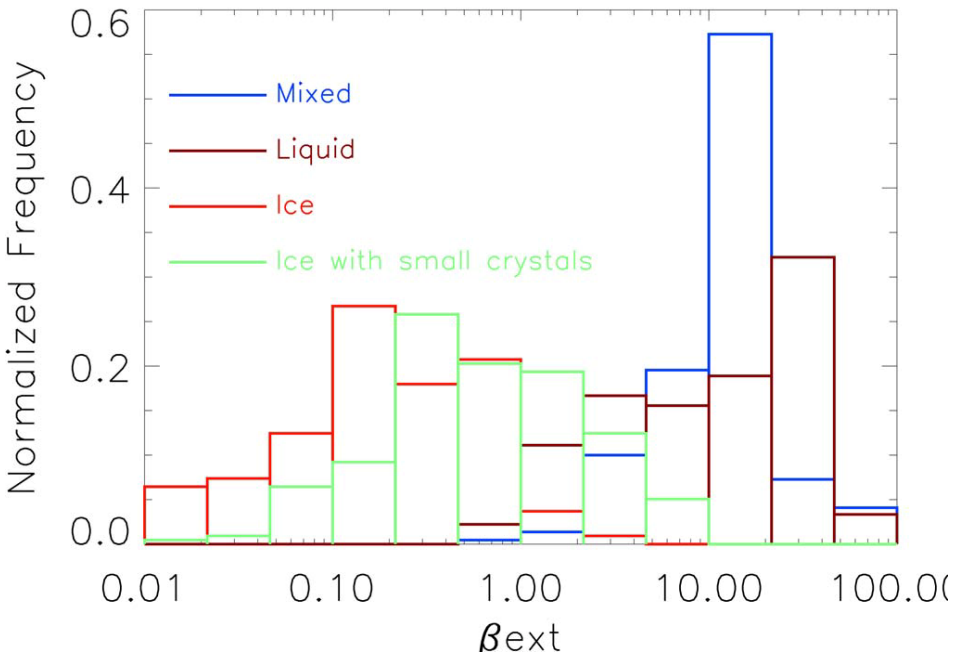

Figure 6. Normalized frequency of occurrence of β_{ext} for mixed-, liquid-, and ice-phase clouds with and without contributions of small ice crystals measured by the FSSP.

Figure 7 shows the fractional contribution of β_{ext} from water droplets for clouds identified as mixed-phase. β_{ext} is dominated by contributions from water droplets, with ice crystals making only minimal contributions. Parameterizations used in some large-scale models (e.g., Boudala et al. 2002) give f_l as a function of temperature, with values ranging from 1.0 at 0°C to 0.0 at a temperature around – 20°C or so. Asterisks represent the fractional contribution of liquid to β_{ext} that would be predicted from Boudala et al. (2002) parameterization scheme, which predicts that ice contributes substantially larger fractions to β_{ext} than shown by observations. This occurs because the parameterization scheme is also based on observations in ice- and liquid-phase conditions.

Figure 8 shows the frequency of occurrence of g calculated from observations and parameterizations. For the two lowest wavelength (λ) bands, where most solar energy is contained, distributions of g for mixed-phase and liquid-phase clouds are similar because water droplets dominate the mass. The parameterizations differ from the observations because f_l is lower for the parameterizations.

Radiative Transfer Calculations

Radiative transfer calculations are performed to quantify how the clustering of phases, not represented in large-scale parameterizations of average conditions, might affect radiative fluxes. A plane parallel Monte Carlo model (developed by A. Macke 1994) is used to compute fluxes and radiance fields, with β_{ext}, ω_0 and $P(\Theta)$ computed from each PSD observed in a mixed-phase cloud as input. Another series of simulations is performed with the same $\beta_{ext,}$ but with ω_0 and $P(\Theta)$ determined from scattering properties computed from the Boudala et al. (2002) parameterization. Figure 9 compares the top of the atmosphere albedo in 4 solar broad bands for 1 km thick clouds computed using the 2 techniques.

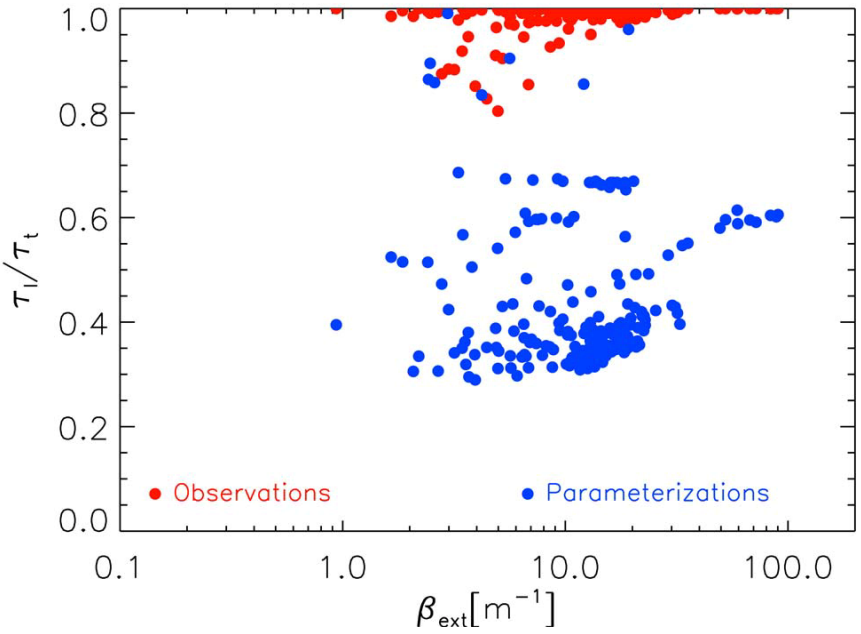

Figure 7. Fraction of β_{ext} due to liquid particles compared to total β_{ext} as function of total β_{ext} for all cloud penetrations identified as mixed-phase. Circles represent calculations using observed PSDs, asterisks represent calculations using the Boudala et al.(2002) parameterization of liquid fraction as described in text.

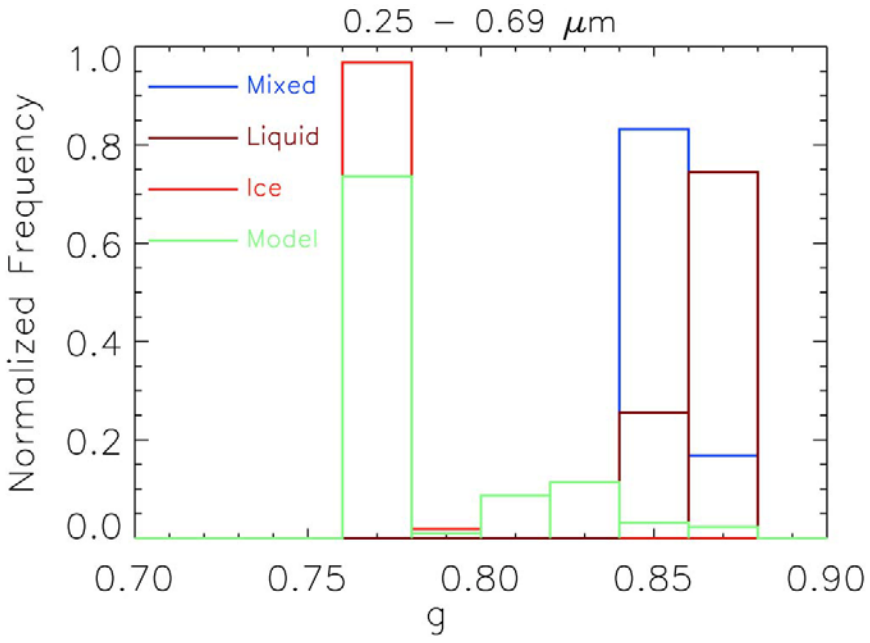

Figure 8. Normalized frequency distributions of g for 4 broad bands commonly used in large-scale models. Different line types correspond to frequency distributions for mixed-phase, liquid-phase, and ice-phase clouds, and for calculations of g using the Boudala et al. (2002) parameterization of liquid water fraction.

Differences in the observed and parameterized albedos are significant because they differ by more than 5%, the flux accuracy criterion identified by Vogelman and Ackerman (1995) as needed for large-scale models. Differences in cloud heating rate profiles would also feedback on cloud water and cloud amount in large-scale model simulations. Although differences in Figure 9 are informative, the most important climatic issue is determining representations for scattering properties over large spatial scales used in GCMs (order 100 km), where mixed-, ice- and water-phase clouds co-exist at temperatures between 0°C and –30°C. Table 1 compares the average albedo in 4 broad bands computed from the observed scattering properties against that calculated using the parameterized scattering properties, where the averages are computed over all mixed-, liquid-, and ice-phase clouds.

For lower λ bands, when using surface albedos corresponding to typical snow-covered surfaces (e.g., 0.7), agreement between simulations using observed and parameterized scattering properties is good as differences in albedo are less than the 5% accuracy criterion identified. For a surface albedo of 0.4 in visible channels, the difference is around 5%. The experiments in Figure 9 and Table 1 seem to reach contradictory conclusions about how well parameterizations used in large-scale models represent mixed-phase scattering properties, especially for cases with high surface albedos. The differences occur because of the scales over which the comparisons are performed, from small scales in Figure 9 to large-scale averages in Table 1. The differences noted in Figure 9 would be more apt to affect albedos averaged over larger scales if the occurrence of particular phases was clustered. Analysis of data from the Convair shows that phases are indeed clustered: over 90% of the 30-s penetrations identified as mixed-phase occur either before or after another mixed-phase cloud distribution.

Discussion and Summary

Analysis of Arctic in-situ microphysical collected during FIRE.ACE and SHEBA show that supercooled water drops generally dominate mass contents of mixed-phase clouds, and hence their single-scattering properties. Since observations show that the occurrence of phases in these clouds is clustered, large-scale averages may not be representative of the climatic effects of mixed-phase clouds. Therefore, for temperature ranges where water and ice may co-exist, an accurate representation of not only the average liquid fraction of clouds, but also of the probability distribution of liquid fraction and the nature of phase clustering is needed for implementation in large-scale models.

Acknowledgments

This research was supported by the Department of Energy Atmospheric Radiation Measurement (ARM) program under grant number DE-FG03-02ER63337. Data from the NCAR C-130 were obtained from the Joint Office of Science Support (JOSS) at UCAR. The cloud microphysical data obtained by the Canadian CV580 were obtained from the NASA Langley Research Center Atmospheric Sciences Data Center. The assistance of Mike Timlin in manuscript preparation was appreciated.

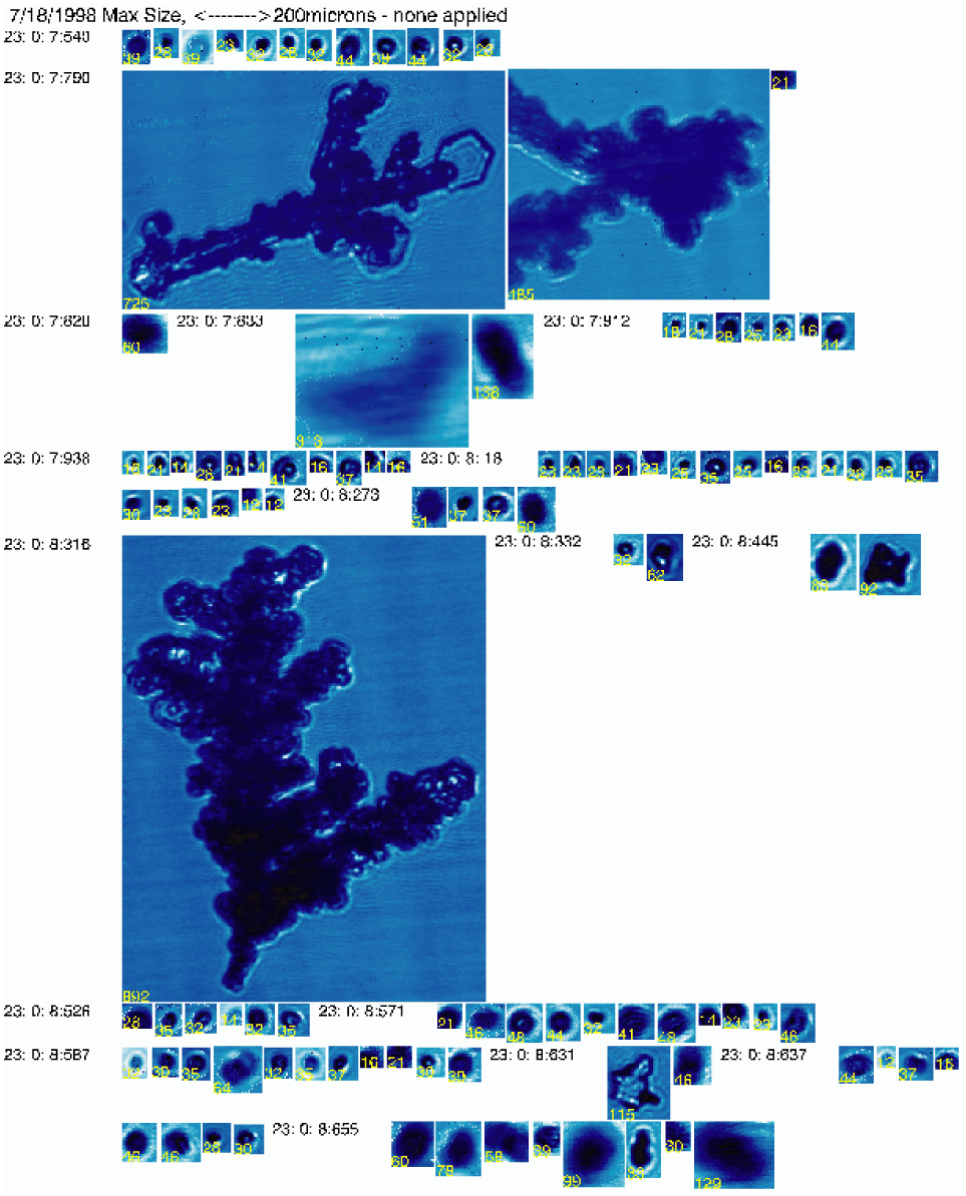

Figure 9. Albedo computed assuming 1 km thick cloud and single-scattering properties determined from observations of mixed-phase clouds from Convair on horizontal axis versus albedo determined from parameterized single-scattering properties on vertical axis. Each point represents calculation from 30-s time average of in-situ measurements.

Table I. Average albedo computed at top of the atmosphere for different λ bands using different estimates of surface albedo (ground) for solar zenith angle of 60°. Different albedos correspond to simulations conducted using observed single-scattering properties and parameterized single-scattering properties.

λ (μm)	R (ground)	Rtoa(observed)	Rtoa(parameterized)
0.25 to 0.69	0.70	0.75	0.77
0.69 to 1.19	0.50	0.64	0.65
1.19 to 2.38	0.10	0.36	0.24
2.38 to 4.00	0.05	0.059	0.045
0.25 to 0.69	0.40	0.58	0.61

References

Boudala, F. S., G. A. Isaac, S. G. Cober, Q. Fu, and A. V. Korolev, 2002b: Parameterization of liquid fraction in terms of temperature and cloud water content in stratiform mixed phase clouds. 11th Conf. Cloud Physics. *Amer. Meteor. Soc*., Ogden, Utah, 2.5.

Cober, S. G., G. A. Isaac, A. V. Korolev, and J. W. Strapp, 2001: Assessing cloud-phase conditions. *J. Appl. Meteor*., **40**, 1967-1983.

McFarquhar, G. M., and S. G. Cober, 2004: Single-scattering properties of mixed phase Arctic clouds at solar wavelengths: impacts on radiative transfer. *J. Climate*, submitted.

Shupe, M. D., T. Uttal, S. Y. Matrosov, and A. S. Frisch, 2001: Cloud water contents and hydrometeor sizes during the FIRE Arctic clouds experiment. *J. Geophys. Res.*, **106**, 15015-15028.

Vogelman, A. M., and T. P. Ackerman, 1995: Relating cirrus cloud properties to observed fluxes: A critical assessment. *J. Atmos. Sci.*, **52**, 4285-4301.

Yang, P., K. N. Liou, K. Wyser, and D. Mitchell, 2000: Parameterization of the scattering and absorption properties of individual ice crystals. *J. Geophys. Res.*, **105**, 4699-4718.